

This is an Open Access document downloaded from ORCA, Cardiff University's institutional repository: <https://orca.cardiff.ac.uk/id/eprint/107680/>

This is the author's version of a work that was submitted to / accepted for publication.

Citation for final published version:

Wenzel, Margot , Meier-Menches, Samuel, Williams, Thomas, Rämisch, Eberhard, Barone, Giampaolo and Casini, Angela 2017. Selective targeting of PARP-1 zinc finger recognition domains with Au(III) organometallics. *Chemical Communications* 54 (6) , pp. 611-614. 10.1039/C7CC08406D

Publishers page: <http://dx.doi.org/10.1039/C7CC08406D>

Please note:

Changes made as a result of publishing processes such as copy-editing, formatting and page numbers may not be reflected in this version. For the definitive version of this publication, please refer to the published source. You are advised to consult the publisher's version if you wish to cite this paper.

This version is being made available in accordance with publisher policies. See <http://orca.cf.ac.uk/policies.html> for usage policies. Copyright and moral rights for publications made available in ORCA are retained by the copyright holders.



# Selective targeting of PARP-1 zinc finger recognition domains with Au(III) organometallics

Margot N. Wenzel,<sup>a</sup> Samuel M. Meier-Menches,<sup>a</sup> Thomas L. Williams,<sup>a</sup> Eberard Rämisch,<sup>b</sup> Giampaolo Barone<sup>c</sup> and Angela Casini<sup>a</sup>

**The binding of Au(III) complexes to the zinc finger domain of the anticancer drug target PARP-1 was studied using a hyphenated mass spectrometry approach combined with quantum mechanics/molecular mechanics (QM/MM) studies. Competition experiments were carried out, whereby each Au complex was exposed to two types of zinc fingers. Notably, the cyclometallated Au-C<sup>^</sup>N complex was identified as the most selective candidate to disrupt the PARP-1 zinc finger domain, forming distinct adducts compared to the coordination compound Auphen.**

Zinc finger domains (ZFs) are relatively small protein structural motifs coordinating Zn<sup>2+</sup> ions and functioning as recognition domains for nucleic acids or proteins. Proteins that contain zinc fingers are classified into several different structural families, playing important roles in cellular functions such as transcription, apoptosis, DNA repair and RNA packaging.<sup>1</sup> A particular ZF domain is determined by its three-dimensional structure, but it can also be recognized based on the primary structure of the peptide or the identity of the ligands coordinating the Zn<sup>2+</sup> ion. The latter are in general Cys<sub>2</sub>His<sub>2</sub> (CCHH), Cys<sub>2</sub>HisCys (CCHC) and Cys<sub>4</sub>-types (CCCC) domains. Notably, the respective protein functions dictate the coordination environment of zinc in the ZF domain. For example, while the zinc fingers of transcription factors involve mainly two cysteines and two histidines (CCHH) coordinating zinc, hormone receptors feature ZFs with four cysteines.<sup>2</sup>

ZF proteins have been shown to be involved in cancer progression, and some of them are promising therapeutic targets.<sup>3</sup> For example, inhibition of the zinc finger protein poly(ADP-ribose)-polymerase-1 (PARP-1), essential in preserving genomic integrity<sup>4, 5</sup> and involved in cisplatin resistance mechanisms,<sup>6</sup> has been recently shown to be a successful strategy to treat cancers bearing BRCA1/2 mutations.<sup>7</sup> In fact, three PARP-1 inhibitors were approved

over the last four years as chemotherapeutic agents targeting the catalytic NAD<sup>+</sup> binding site.<sup>8</sup> In humans, 17 PARP isoforms have been identified so far, all featuring a similar C-terminal catalytic domain<sup>9</sup> and consequently, inhibitors of the catalytic function of PARP-1 can also interact with other isoforms,<sup>5</sup> leading to severe side effects.<sup>10</sup> As an alternative strategy, since PARP-1 is the only isoform containing two N-terminal ZF domains,<sup>11</sup> its selective inhibition may be achieved by disrupting the specific CCHC zinc finger domains and thereby, the protein–DNA interaction.

Within this framework, we have demonstrated the possibility to potentially inhibit PARP-1 using Au(III) compounds targeting its ZF motif. Thus, both the coordination complex [Au(phen)Cl<sub>2</sub>]Cl (phen = 1,10-phenanthroline, Auphen)<sup>12</sup> and the organometallic cyclometalated compound [Au(py<sup>b</sup>-H)Cl<sub>2</sub>] (py<sup>b</sup> = 2-benzylpyridine, Au-C<sup>^</sup>N)<sup>13</sup> (Figure 1A) inhibited PARP-1 *in vitro* at a nM level, which is an order of magnitude higher than that of the FDA-approved drug Olaparib (IC<sub>50</sub> = 0.03 ± 0.01 μM).<sup>14</sup> Furthermore, we postulated a mechanism of inhibition by Auphen involving a transmetallation reaction, whereby Au<sup>3+</sup> ions replace Zn<sup>2+</sup> in the ZF, forming the so-called *gold-finger*,<sup>12</sup> and disrupting the DNA binding properties of PARP-1.

So far, gold-finger formation was mainly assessed by mass spectrometry (MS) techniques.<sup>2, 12, 15-17</sup> Recently, Farrell *et al.* investigated the binding of coordination Au(III)/Au(I) complexes to the ZF of the HIV-nucleocapsid protein (NCp7) by high resolution and traveling-wave ion mobility mass spectrometry, respectively.<sup>17-19</sup> Despite these encouraging results, doubts remain on the selectivity of anticancer Au(III) compounds for discriminating between CCHC over CCHH or CCCC coordination motifs, as such compounds were shown to interact with CCHH and CCCC zinc fingers alike, when incubated individually.<sup>2, 15</sup>

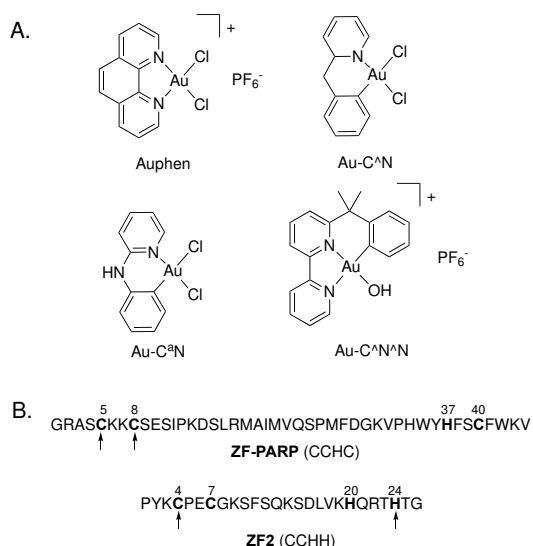


**Figure 1.** A. Scheme of the four Au(III) complexes used in this study; B. Sequences of the CCHC (top) and CCHH (bottom) model peptides of zinc fingers (ZF-PARP and ZF-2, respectively). Arrows indicate the confirmed binding site of gold from the tandem mass spectrometry experiments.

Sampling the metallodrug binding selectivity for intact protein domains under “competitive” conditions - such as those encountered in a cellular context - represents a considerable experimental challenge,<sup>20</sup> which is mainly caused by the difficulty of separating the intact reaction products, by potential ligand scrambling reactions and by redox reactivity during lengthy work-up and analysis. Thus, we report here on a rapid hyphenated mass spectrometry approach to assess: (i) the binding preference of representative Au(III) complexes towards the CCHC PARP-1-like zinc finger domain and (ii) the coordination sphere of gold ions upon binding to ZF domains.

To these aims, three representative cyclometalated Au(III) complexes featuring C<sup>N</sup> and C<sup>N</sup>N type of ligands (Figure 1A) were tested for their selectivity towards the CCHC ZF domains in comparison to Auphen. Interestingly, [Au(bipy<sup>dmb</sup>-H)(OH)][PF<sub>6</sub>] (bipy<sup>dmb</sup> = 6-(1,1-dimethylbenzyl)-2,2'-bipyridine, Au-C<sup>N</sup>N) showed stability in physiological media and moderate cytotoxic activity towards both cisplatin-sensitive and resistant cancer cell lines.<sup>21</sup> Moreover, [Au(phepy<sup>a</sup>-H)Cl<sub>2</sub>] (phepy<sup>a</sup> = N-phenylpyridin-2-amine, Au-C<sup>N</sup>), also reported as a moderate cytotoxic agent,<sup>22</sup> is structurally very similar to Au-C<sup>N</sup>. The MS analysis was carried out using peptide sequences of the N-terminal CCHC zinc finger domain of PARP-1 (ZF-PARP, 44 amino acids, Figure 1B) previously used by us,<sup>12</sup> and of the CCHH zinc finger as a model for transcription factors (ZF2, 26 residues, Figure 1B),<sup>15</sup> both reduced with dithiothreitol (DTT) and incubated with zinc acetate in (NH<sub>4</sub>)<sub>2</sub>CO<sub>3</sub> buffer (25 mM, pH 7.4) in order to form the ZF motifs prior to exposure to the gold compounds.

Initially, individual experiments were carried out, whereby each gold complex was incubated separately with each type of ZF peptide in a 3:1 ratio (see Supporting Information, Figures S1-S4 and Tables S1-S4). The results showed that all compounds react quickly, but distinctively, with both types of

ZF domains by displacing zinc from the coordination site. Overall, while Auphen forms gold-finger domains upon release of the phen ligand with both ZFs, the cyclometalated complexes mostly retain the C<sup>N</sup> or C<sup>N</sup>N ligands stabilizing the Au(III) oxidation state in the resulting adducts.

A HPLC-ESI-MS method was then set up for performing the competition experiments. Each gold complex was assessed for its binding preference for one type of zinc finger motif when exposed to both CCHH and CCHC ZF peptides. To this end, each compound was shortly incubated with an equimolar mixture of ZF-PARP and ZF2. In order to reduce the probability of on-column ligand exchange or possible demetalation reactions, a 10 min linear gradient up to 95% MeCN was used and separation was performed using a C4 column (300 Å). The intact and unreacted ZF domains were well separated under these conditions and eluted at 3.08 min (ZF2) and 5.24 min (ZF-PARP), respectively (Figures S1 and S2). Thus, ZF2 was detected at *m/z* 494.5862 (*m*<sub>theor</sub> = 494.5781, *z* = 6+) and ZF-PARP was detected at *m/z* 732.5150 (*m*<sub>theor</sub> = 732.5078, *z* = 7+).

The binding preference of the compounds towards ZF-PARP over ZF2 was then calculated by assuming that the ionization efficiency of the gold-adducts, *i.e.* gold finger, is similar to the corresponding unreacted zinc finger. Percentages of gold-adduct formation are obtained for ZF-PARP and ZF2 separately, by summing up the attributable peak areas obtained from the extracted ion chromatograms (EIC) of each unreacted ZF-domain and the respective interaction products (see experimental for details and Table S11). The affinity for gold binding to the ZF-PARP vs ZF2 is then expressed as a ratio of the two percentages for forming gold-adducts, termed binding preference ratio (BPR). The higher the BPR for a given compound, the more pronounced is its affinity for ZF-PARP. Thus, the incubation of the mixture of both ZFs with Auphen revealed replacement of Zn by Au in the ZF domains next to unreacted ZF2 and ZF-PARP. The interaction product between Auphen and ZF2 was found at 3.26 min corresponding to [Apo-ZF2+Au<sup>I</sup>-H]<sup>6+</sup> (Figures 2A and S5 and Table S5). At an elution time of 5.29 min, the mass spectrum obtained from the broad peak identified [Apo-ZF-PARP+Au<sup>I</sup>-H]<sup>7+</sup> as the main interaction product. A BPR of 29 in favour of ZF-PARP was obtained for Auphen.

The organometallic Au(III) complexes were tested in an analogous setting. Upon incubation of Au-C<sup>N</sup> with an equimolar mixture of both peptides for 5 min, Apo-ZF2 was detected (elution at 3.11 min), as well as the corresponding adduct [Apo-ZF2+Au<sup>I</sup>-H]<sup>n+</sup> at 3.26 min (Figures 2B, S6A and S6B and Table S6). Apo-ZF-PARP was detected at 5.26-5.48 min, while the main adducts were identified as [Apo-ZF-PARP+Au<sup>III</sup>C<sup>N</sup>-2H]<sup>7+</sup> and [Apo-ZF-PARP+2[Au<sup>III</sup>C<sup>N</sup>-2H]]<sup>7+</sup> overlapping in time with the unreacted ZF-PARP (Figure S6B). Au-C<sup>N</sup> showed the highest selectivity for the CCHC type of ZF with a BPR of 32, even though the gold organometallic reacts equally fast with both model peptides individually (Figures S3 and S4). It should be noted that another peak was observed at 4.96 min, identified as an adduct of the Au-C<sup>N</sup> complex with DTT (Figure S6A).

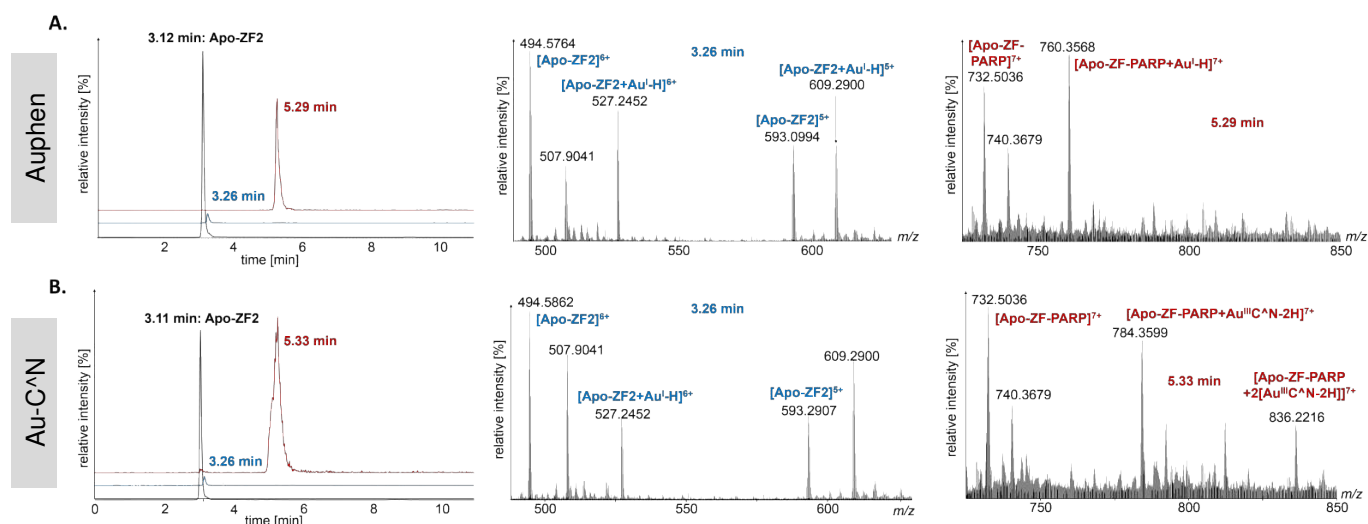


**Figure 2.** **A.** Extracted chromatograms of the HPLC-ESI-MS analysis of the reaction of Auphen with ZF-PARP and ZF2 (3:1:1 ratio) after 5 min incubation at 37°C and corresponding mass spectra at 3.26 and 5.29 min; **B.** Extracted chromatograms of the HPLC-ESI-MS analysis of the reaction of Au-C<sup>N</sup> with ZF-PARP and ZF2 (3:1:1 ratio) after 5 min incubation at 37°C and corresponding mass spectra at 3.26 and 5.33 min.

In the competition experiment, whereby Au-C<sup>N</sup> was incubated with both ZF2 and ZF-PARP, a new peak at 3.82 min indicated the presence of an adduct of the type [Apo-ZF2+Au<sup>III</sup>C<sup>N</sup>-2H]<sup>n+</sup> and confirming a different reactivity with respect to Au-C<sup>N</sup> (Figure S7 and Table S7). The mass spectrum obtained from the broad peak at 5.28 min indicated the predominant presence of the Apo-ZF-PARP peptide, along with the corresponding adduct [Apo-ZF-PARP+Au<sup>III</sup>C<sup>N</sup>-2H]. Remarkably, the obtained results clearly showed that Au-C<sup>N</sup> and Au-C<sup>N</sup>, although structurally very similar, shows a low selectivity towards the CCHC type ZF (BPR of 2).

Finally, incubation of the Au-C<sup>N</sup> complex resulted in the formation of adducts with both peptides (Figure S8 and Table S8) and selective towards the CCHC type of ZFs (BPR of 10). Specifically, adducts eluting at 3.26 min were identified as mono- and bis-Au(I) adducts on Apo-ZF2, whereas [Apo-ZF-PARP+Au<sup>III</sup>-3H] and [Apo-ZF-PARP+Au<sup>III</sup>C<sup>N</sup>-3H] were detected at 5.24 minutes, alongside Apo-ZF-PARP, in line with the individual experiments (Figures S3 and S4). Thus, although displacing Zn from the peptide, a monodentate binding mode to the ZF does not entail an appreciable gain in selectivity.

The second series of competition experiments was designed to evaluate the selectivity of Auphen and Au-C<sup>N</sup> for the CCHC type of ZFs in presence of other proteins. Cytochrome c (cyt c), a small heme-containing protein, was selected for this study as a suitable model for LC-MS experiments.<sup>23, 24</sup> Each gold complex was incubated with a 1:1 mixture of ZF-PARP and cyt c for 5 min at 37°C and analysed using the same HPLC-ESI-MS set-up. In all cases, no gold adducts were observed with cyt c, whereas adducts with ZF-PARP were identified as similar than in the individual experiments, *i.e.* Au(I) ions with Auphen and formation of [Apo-ZF-PARP+Au<sup>III</sup>-C<sup>N</sup>-2H] adducts with Au-C<sup>N</sup> (Figures S9-S10 and Tables S9-S10). Similar results were obtained replacing

cyt c with another model protein, namely ubiquitin (data not shown). This result confirmed the selectivity of Auphen and Au-C<sup>N</sup> for the CCHC type ZF, also in presence of other proteins and excludes purely non-selective coordination of the metal to surface-exposed and nucleophilic amino acids.

Tentative identification of the binding sites of the two most promising gold complexes (Auphen and Au-C<sup>N</sup>) was then conducted using an online top-down approach. Fragmentation experiments by collision-induced dissociation (CID) were carried out on selected adducts from the individual or competition experiments, allowing the production of b and y ions fragments on both peptides and identification of the metallated residues. The isolated adducts corresponded to [Apo-ZF2+Au<sup>I</sup>-H] and [Apo-ZF-PARP+Au<sup>III</sup>-3H] in the case of Auphen (Figures S3 and S4), and [Apo-ZF2+Au<sup>III</sup>C<sup>N</sup>-2H] and [Apo-ZF-PARP+Au<sup>III</sup>C<sup>N</sup>-2H] in the case of Au-C<sup>N</sup> (Figures 2, S4 and S6). Figure S11 shows the identified metallated fragments and binding sites for each type of adduct. For [Apo-ZF2+Au<sup>I</sup>-H], Cys4 (Figure 1B) was confirmed as the most stable Au-binding site. Furthermore, the presence of a  $\gamma_7$  fragment suggested that one of the two histidine residues (His20 or His24, Figure 1B) might also be involved in coordinating the Au<sup>I</sup> ion. The fragmentation pattern of [Apo-ZF2+Au<sup>III</sup>C<sup>N</sup>-2H] suggested a similar reactivity involving Au(C<sup>N</sup>) coordinating to Cys4/7 and His24. On ZF-PARP, only b fragments were identified in both cases. The presence of a metallated b<sub>7</sub> fragment indicated that Cys5 (Figure 1B) was a binding site for the Au(I) ion of Auphen. In the case of Au-C<sup>N</sup>, the first metallated fragment identified was b<sub>12</sub>, therefore suggesting Cys5 or Cys8 as likely binding sites. Complementary ion mobility mass spectrometry (IM-MS) studies were conducted to assess the structure of the gold finger in the case of Au-C<sup>N</sup> (Figure S12) and suggest extensive unfolding of the peptide upon adduct formation as shown by the similar drift times as for the Apo-ZF-PARP in the applied experimental conditions.

To provide an atomistic support to the experimental results, DFT calculations have been performed to evaluate the binding energy of compounds Au-C<sup>N</sup>, Au-C<sup>N</sup> and Au-C<sup>N</sup> (See SI for details). The obtained results (Figures S13-S16, Table S12) showed that the binding with cysteinato (Cys<sup>-</sup>), after substitution of one chlorido ligand, is highly preferred



compared to the binding with histidine, the latter being characterized by positive calculated energy values of adduct formation. Moreover, the binding of both Au-C<sup>^</sup>N and Au-C<sup>^</sup>N with two Cys<sup>-</sup> ligands is much stronger than that with only one Cys<sup>-</sup>, as in the case of the Au-C<sup>^</sup>N<sup>^</sup>N, or with two mixed Cys<sup>-</sup>/His ligands.

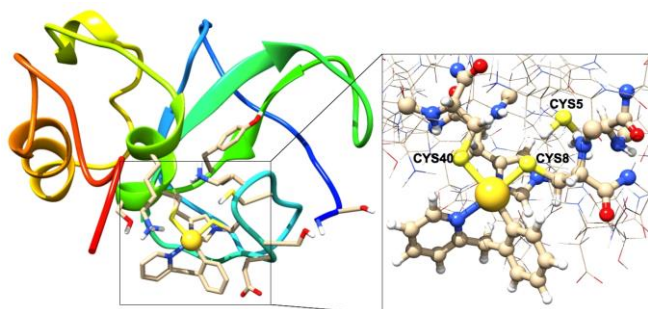


**Figure 3.** Gold finger formation. Example of the possible binding of Au-C<sup>^</sup>N with the zinc finger domain of PARP-1, in which two chlorido ligands of Au-C<sup>^</sup>N have been replaced by two cysteinato groups. Represented is the most stable structure among four isomers considered (see Figure S17) obtained by QM/MM calculations, after full geometry optimization. In the enlarged picture, the QM layer is highlighted in balls and sticks and the Au<sup>3+</sup> ion as a yellow sphere. Drawings produced by the UCSF Chimera package.<sup>25</sup>

Finally, the binding Au-C<sup>^</sup>N with two Cys<sup>-</sup> is also slightly stronger than that established by Au-C<sup>^</sup>N. These results prompted us to hypothesize a possible binding mechanism of Au-C<sup>^</sup>N with the zinc finger domain of PARP-1. QM/MM calculations (see SI for details) have been performed using the ZF-PARP model (PDB ID 2DMJ). By removing the zinc ion from the CCHC coordination site, it has been verified that Au-C<sup>^</sup>N can easily approach it in four different stereochemical isomers (Figures S17-S19). Specifically, the two accessible Cys residues, Cys8 and Cys40, can coordinate the Au<sup>3+</sup> ion, while the C<sup>^</sup>N ligand remains outside the protein cavity (Figure 3). Instead, Cys5 is unlikely to bind gold, since this residue is more buried in the folded peptide. These results are in line with our top-down analysis and those recently reported by Farrell *et al.* on the binding of an Au(I) complex to another CCHC ZF model.<sup>18</sup>

In summary, we have set-up a rapid hyphenated HPLC-ESI-MS approach to study the reactivity and selectivity of a series of Au(III) complexes towards model peptides of zinc fingers. The nature of the adducts formed were identified and showed that even though all gold complexes are very reactive towards both types of zinc fingers (CCHH and CCHC) individually, trends in selectivity can be drawn. Firstly, both the organometallic Au-C<sup>^</sup>N compound and the coordination complex Auphen exhibited a significant selectivity for the PARP-1 ZF also in the presence of a CCHH type of ZF domain, representing a rather unique feature in the quest for selective PARP-1 inhibitors. Furthermore, the Au-C<sup>^</sup>N complex has been able of preserving the Au<sup>3+</sup> oxidation state while retaining the C<sup>^</sup>N ligand upon binding to the most accessible Cys residues. Thus, leading to important alterations of the DNA recognition domain of PARP-1 and eventually to protein inhibition.<sup>13,15</sup> Notably, while Au(III) coordination complexes as Auphen have been previously shown to bind also to the membrane water and glycerol channels aquaporins, Au-C<sup>^</sup>N was scarcely reactive, thus, holding even more promise to selectively target ZF domains.<sup>26</sup> Overall, targeting the structural DNA recognition domain of PARP-1 instead of the catalytic domain, similar in several PARP isoforms, appears as a promising strategy to increase the selectivity of PARP-1 inhibitors.

## Conflicts of interest

There are no conflicts to declare.

## References

1. A. Klug, *Ann. Rev. Biochem.*, 2010, **79**, 213-231.
2. A. Jacques, C. Lebrun, A. Casini, I. Kieffer, O. Proux, J.-M. Latour and O. Sénèque, *Inorg. Chem.*, 2015, **54**, 4104-4113.
3. J. Jen and Y.-C. Wang, *J. Biomed. Sci.*, 2016, **23**, 53.
4. M. Rouleau, A. Patel, M. J. Hendzel, S. H. Kaufmann and G. G. Poirier, *Nat. Rev. Cancer*, 2010, **10**, 293-301.
5. J. D. Steffen, J. R. Brody, R. S. Armen and J. M. Pascal, *Frontiers Oncol.*, 2013, **3**, 301.
6. G. Zhu, P. Chang and S. J. Lippard, *Biochemistry*, 2010, **49**, 6177-6183.
7. K. Y. Lin and W. L. Kraus, *Cell*, 2017, **169**, 183.
8. C. J. Lord and A. Ashworth, *Science*, 2017, **355**, 1152-1158.
9. V. Schreiber, F. Dantzer, J.-C. Ame and G. de Murcia, *Nat. Rev. Mol. Cell Biol.*, 2006, **7**, 517-528.
10. M. Friedlander, S. Banerjee, L. Mileskin, C. Scott, C. Shannon and J. Goh, *As. J. Clin. Oncol.*, 2016, **12**, 323-331.
11. K. Bossak, W. Goch, K. Piątek, T. Frączyk, J. Poznański, A. Bonna, C. Keil, A. Hartwig and W. Bal, *Chem. Res. Toxicol.*, 2015, **28**, 191-201.
12. F. Mendes, M. Groessler, A. A. Nazarov, Y. O. Tsybin, G. Sava, I. Santos, P. J. Dyson and A. Casini, *J. Med. Chem.*, 2011, **54**, 2196-2206.
13. B. Bertrand, S. Spreckelmeyer, E. Bodio, F. Cocco, M. Picquet, P. Richard, P. Le Gendre, C. Orvig, M. A. Cinellu and A. Casini, *Dalton Trans.*, 2015, **44**, 11911-11918.
14. M. Niu and Y. Gu, *New J. Chem.*, 2015, **39**, 1060-1066.
15. U. A. Laskay, C. Garino, Y. O. Tsybin, L. Salassa and A. Casini, *Chem. Comm.*, 2015, **51**, 1612-1615.
16. C. Abbehausen, E. J. Peterson, R. E. F. de Paiva, P. P. Corbi, A. L. B. Formiga, Y. Qu and N. P. Farrell, *Inorg. Chem.*, 2013, **52**, 11280-11287.
17. S. R. Spell, J. B. Mangrum, E. J. Peterson, D. Fabris, R. Ptak and N. P. Farrell, *Chem. Comm.*, 2017, **53**, 91-94.
18. Z. Du, R. E. de Paiva, K. Nelson and N. P. Farrell, *Angew. Chem. Intl. Ed.*, 2017, **56**, 4464-4467.
19. R. E. F. de Paiva, Z. Du, E. J. Peterson, P. P. Corbi and N. P. Farrell, *Inorg. Chem.*, 2017, **56**, 12308-12318.
20. C. Artner, H. U. Holtkamp, W. Kandioller, C. G. Hartinger, S. M. Meier-Menches and B. K. Keppler, *Chem. Comm.*, 2017, **53**, 8002-8005.
21. G. Marcon, S. Carotti, M. Coronello, L. Messori, E. Mini, P. Orioli, T. Mazzei, M. A. Cinellu and G. Minghetti, *J. Med. Chem.*, 2002, **45**, 1672-1677.
22. Y. Zhu, B. R. Cameron, R. Mosi, V. Anastassov, J. Cox, L. Qin, Z. Santucci, M. Metz, R. T. Skerlj and S. P. Fricker, *J. Inorg. Biochem.*, 2011, **105**, 754-762.
23. M. Wenzel and A. Casini, *Coord. Chem. Rev.*, 2017, DOI: 10.1016/j.ccr.2017.02.012.
24. S. M. Meier, C. Gerner, B. K. Keppler, M. A. Cinellu and A. Casini, *Inorg. Chem.*, 2016, **55**, 4248-4259.
25. E. F. Pettersen, T. D. Goddard, C. C. Huang, G. S. Couch, D. M. Greenblatt, E. C. Meng and T. E. Ferrin, *J. Comput. Chem.*, 2004, **25**, 1605-1612.
26. A. de Almeida, A. F. Mosca, D. Wragg, M. Wenzel, P. Kavanagh, G. Barone, S. Leoni, G. Soveral and A. Casini, *Chem. Comm.*, 2017, **53**, 3830-3833.